**Supplemental Table of Contents:**

Supplemental Figure 1: Histopathological analysis of 20 strains of male and female F1 transgenic.
Supplemental Figure 2: Blood Urea Nitrogen of the transgenic female and male mice strains correlates with histopathology.
Supplemental Figure 3: NGAL measured in the urine of the transgenic female and male mice strains correlates with histopathology.
Supplemental Figure 4: Manhattan plots for the loci influencing the glomerulosclerosis phenotypes of the Tg-F1 mice.
Supplemental Figure 5: Manhattan plots for the loci influencing the casts phenotypes of the Tg-F1 mice.
Supplemental Figure 6: Manhattan plots for the loci influencing the tubular atrophy and interstitial fibrosis phenotypes of the Tg-F1 mice.
Supplemental Figure 7: Manhattan plots for the loci influencing the interstitial inflammation phenotypes of the Tg-F1 mice.
Supplemental Figure 8: Differential expression of the genes located in suggestive loci.
Supplemental Figure 9: Mouse kidney tissue mRNA expression by snRNA-seq of the genes located in the identifies locus on Chr 13.
Supplemental Figure 10: Immunostaining of kidney tissue of the genes identified in the QTL on chromosome 13.
Supplemental Figure 11: Single cell sequencing of TgFVB kidney.
Supplemental Figure 12: Quantitative RT-PCR analysis of genes identified within the Chr. 13 locus.

Supplemental Table 1: Numbers of Tg-F1-mice for each strain
Supplemental Table 2: Primers for the RT-PCR.
Supplemental Table 3. Statistical analysis of the glomerulosclerosis score between the different F1 hybrids compared to Tg-C57BL6/10J mice.
Supplemental Table 4. Statistical analysis of the glomerulosclerosis score between the different F1 hybrids compared to Tg-FVB/NJ mice.

Supplemental Table 5. Statistical analysis of the casts score between the different F1 hybrids compared to Tg-C57BL6/10J mice.
Supplemental Table 6. Statistical analysis of the Casts score between the different F1 hybrids compared to Tg-FVB/NJ mice.
Supplemental Table 7. Statistical analysis of the Tubular Atrophy and Interstitial Fibrosis score between the different F1 hybrids compared to Tg-C57BL6/10J mice.
Supplemental Table 8. Statistical analysis of the Tubular Atrophy and Interstitial Fibrosis score between the different F1 hybrids compared to Tg-FVB/NJ mice.
Supplemental Table 9. Statistical analysis of the Interstitial Inflammation score between the different F1 hybrids compared to Tg-C57BL6/10J mice.
Supplemental Table 10. Statistical analysis of the Interstitial Inflammation score between the different F1 hybrids compared to Tg-FVB/NJ mice.
Supplemental Table 11: Estimated heritability for the kidney pathology scores and BUN
Supplemental Table 12: Suggestive signals (Chromosome Wise Significant) of the glomerulosclerosis scores from the HIV-1 transgenic mice.
Supplemental Table 13: Selection of priority genes in the locus identified on Chr.13.

**Supplementary Figure 1**

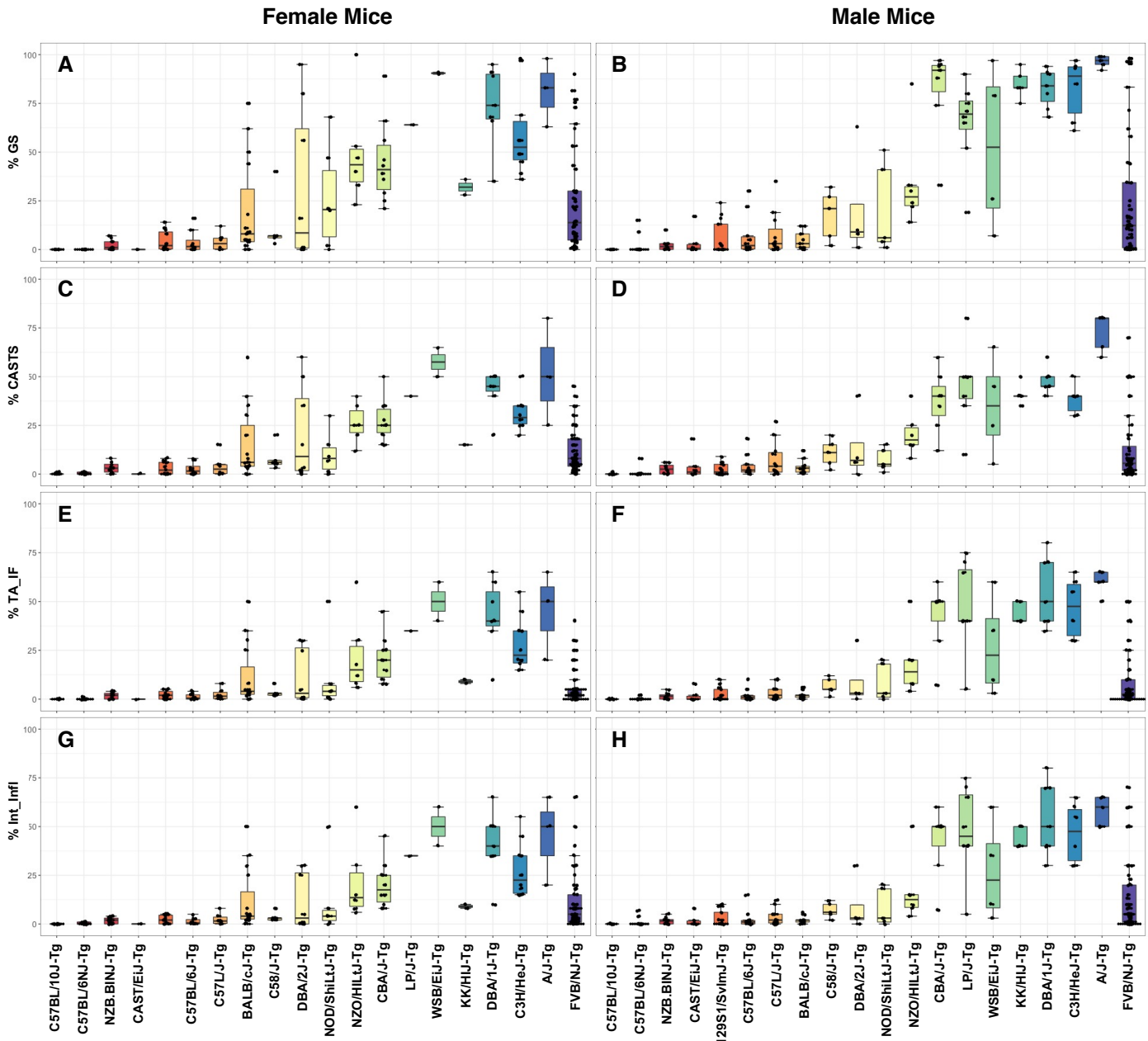


**Supplemental Figure 1 (for Figure 1): Histopathological analysis of 20 strains of male and female F1 transgenic.** (A) Percentage of GS in the kidneys Tg-F1 female mice. (B) Percentage of GS in the kidneys Tg-F1 male mice. (C) Percentage of casts in the kidneys of Tg-F1 female mice. (D) Percentage of casts in the kidneys of Tg-F1 male mice. (E) Percentage cortical area with tubular atrophy/interstitial fibrosis in the kidneys Tg-F1 female mice. (F) Percentage cortical area with tubular atrophy/interstitial fibrosis in the kidneys Tg-F1 male mice. (G) Percentage cortical area with interstitial inflammation in the kidneys Tg-F1 female mice. (H) Percentage of cortical area with interstitial inflammation in the kidneys of Tg-F1 male mice.

# Supplementary Figure 2

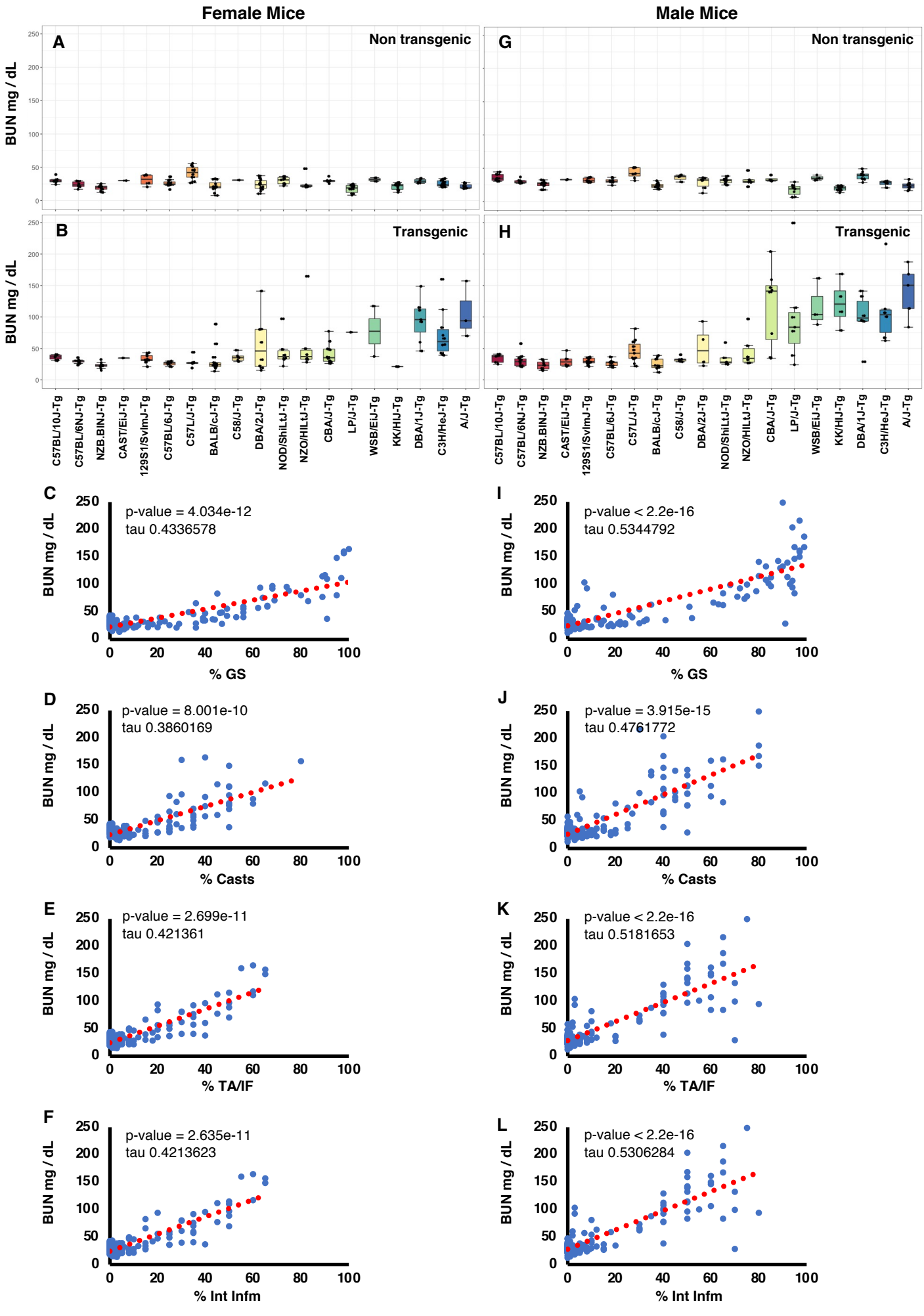

**Supplemental Figure 2 (for Figure 1): Blood Urea Nitrogen of the transgenic female and male mice strains correlates with histopathology.** (A) Baseline BUN in female F1 non-transgenic mice. (B) BUN in female F1-transgenic mice. (C) Increased BUN correlates with the percentage of GS in female mice, P value < 0.001, tau = 0.43, Kendell correlation. (D) Increased BUN correlates with the percentage of casts in female mice, P value < 0.001, tau = 0.38, Kendell correlation. (E) Increased BUN correlates with the percentage of tubular atrophy/interstitial fibrosis in female mice, P value < 0.001, tau = 0.42, Kendell correlation. (F) Increased BUN correlates with the percentage of interstitial inflammation in female mice, P value < 0.001, tau = 0.42, Kendell correlation. (G) Baseline BUN in male F1 non-transgenic mice. (H) BUN in male F1-transgenic mice. (I) Increased BUN correlates with the percentage of GS in male mice, P value < 0.001, tau = 0.53, Kendell correlation. (J) Increased BUN correlates with the percentage of casts in male mice, P value < 0.001, tau = 0.47, Kendell correlation. (K) Increased BUN correlates with the percentage of tubular atrophy/interstitial fibrosis in male mice, P value < 0.001, tau = 0.51, Kendell correlation. (L) Increased BUN correlates with the percentage of interstitial inflammation in male mice, P value < 0.001, tau = 0.53, Kendell correlation

# Supplementary Figure 3

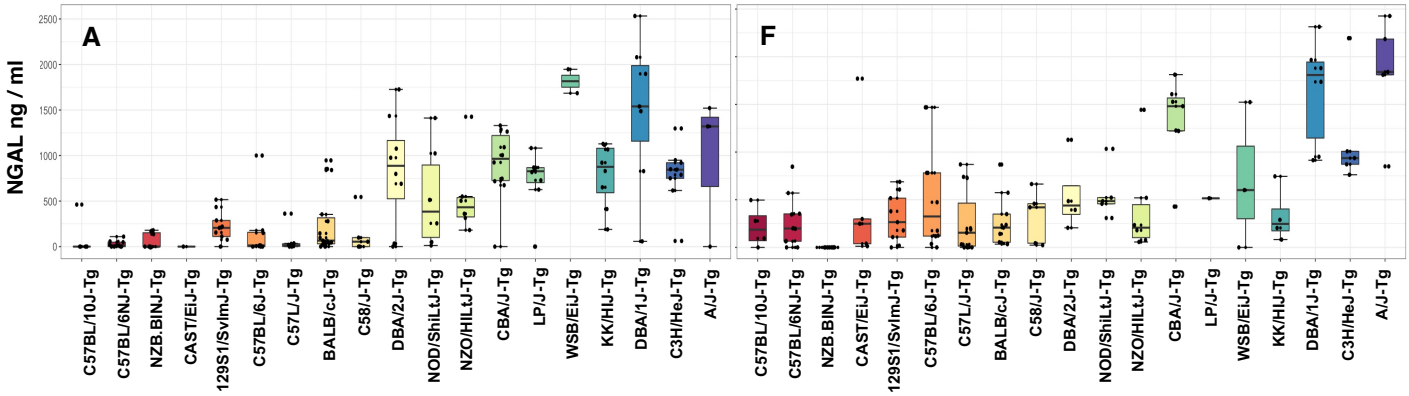


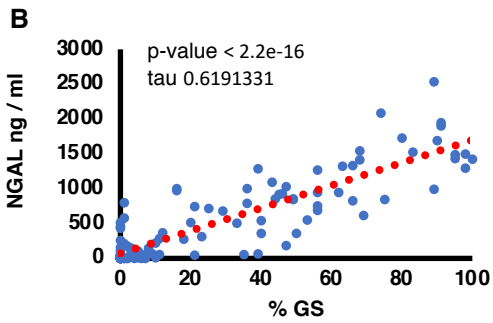


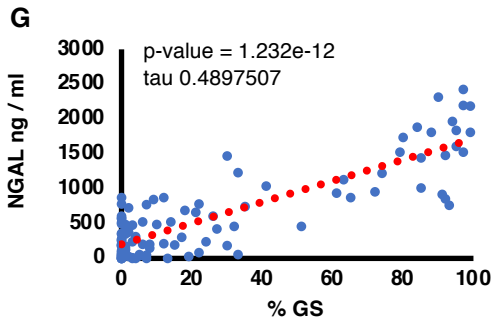


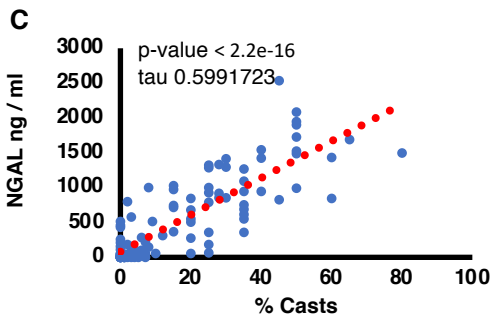


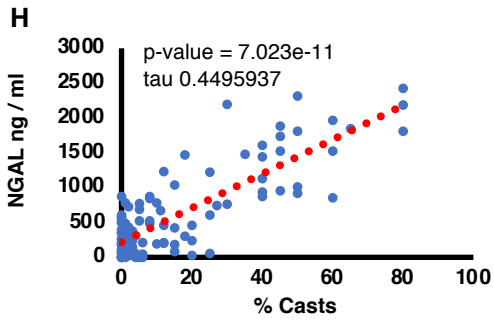


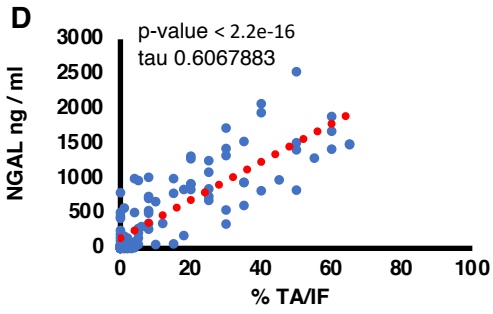


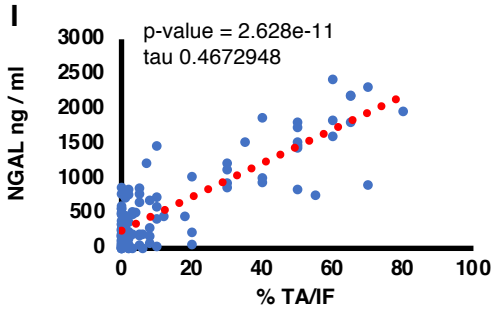


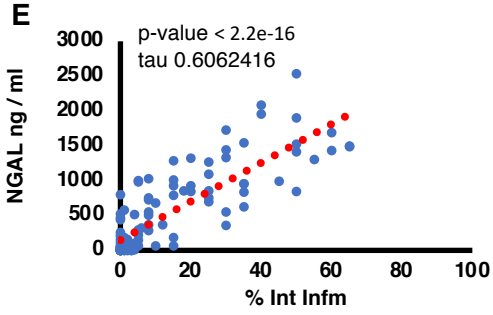


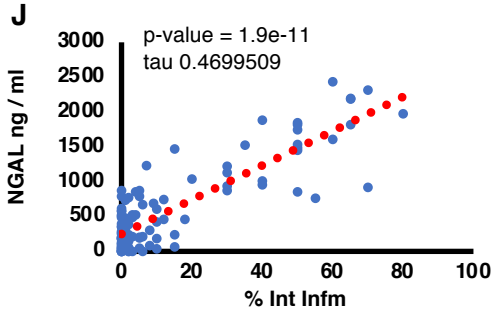

**Supplemental Figure 3 (for Figure 1): NGAL measured in the urine of the transgenic female and male mice strains correlates with histopathology.** (A) NGAL in female F1-transgenic mice**.** (B) Increased NGAL correlates with the percentage of GS in female Tg-mice, P value < 0.001, tau = 0.61, Kendell correlation. (C) Increased NGAL correlates with the percentage of casts in female Tg-mice, P value < 0.001, tau = 0.59, Kendell correlation. (D) Increased NGAL correlates with the percentage of tubular atrophy/interstitial fibrosis in female Tg-mice, P value < 0.001, tau = 0.602, Kendell correlation. (E) Increased NGAL correlates with the percentage of interstitial inflammation in female Tg-mice, P value < 0.001, tau = 0.606, Kendell correlation. (F) NGAL in male F1-transgenic mice. (G) Increased NGAL correlates with the percentage of GS in male Tg-mice, P value < 0.001, tau = 0.48, Kendell correlation. (H) Increased NGAL correlates with the percentage of casts in male Tg-mice, P value < 0.001, tau = 0.44, Kendell correlation. (I) Increased NGAL correlates with the percentage of tubular atrophy/interstitial fibrosis in male Tg-mice, P value < 0.001, tau = 0.46, Kendell correlation. (J) Increased NGAL correlates with the percentage of interstitial inflammation in male Tg-mice, P value < 0.001, tau = 0.46, Kendell correlation. Kendell correlation was used because the data were not equally distributed.

**Supplementary Figure 4**

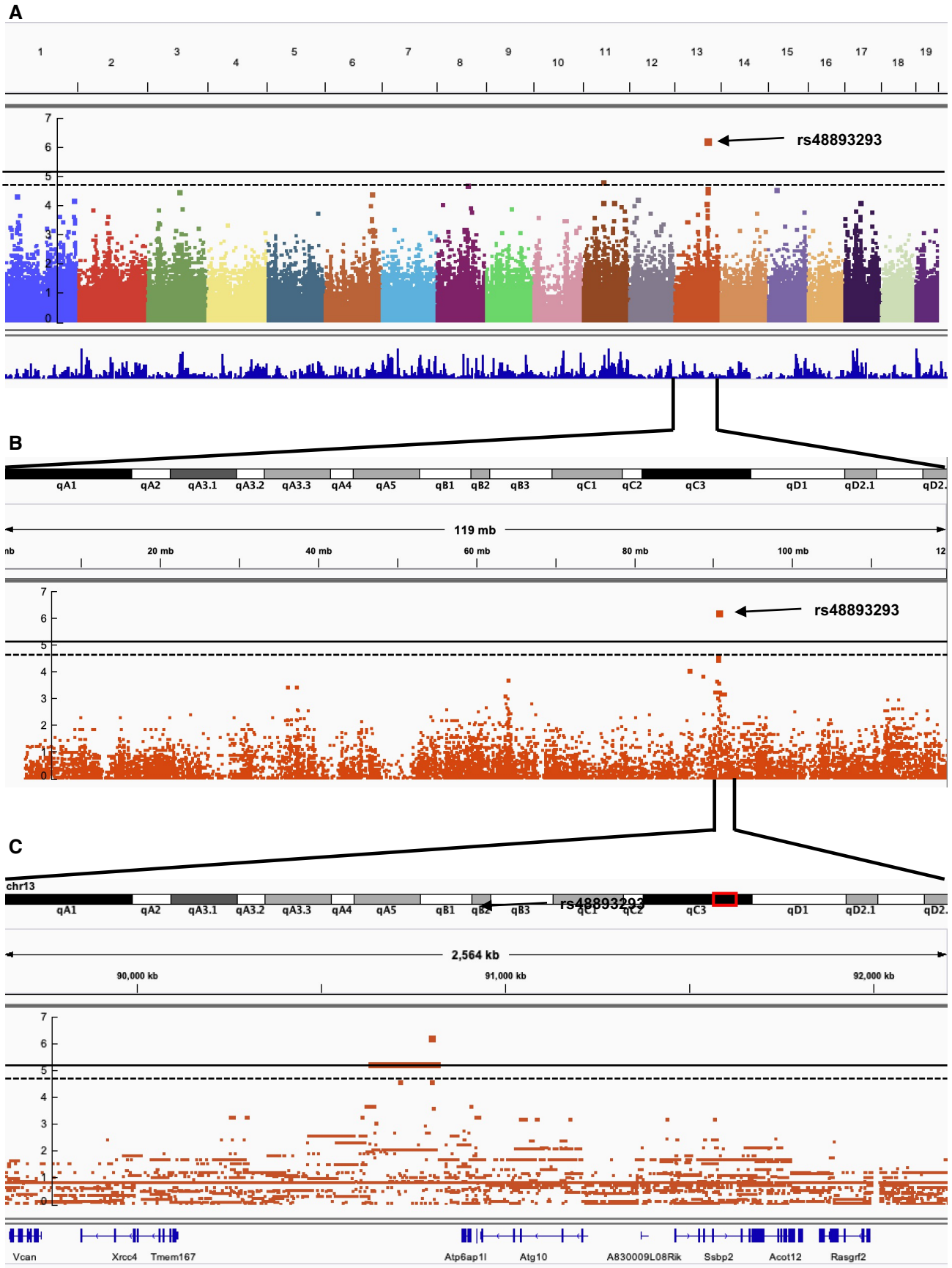

**Supplemental Figure 4: Manhattan plots for the loci influencing the glomerulosclerosis phenotypes of the Tg-F1 mice.** (A) Manhattan plot of the percentage glomerulosclerosis demonstrating a genome-wide significant SNP on Chr13. (B) Manhattan plot of Chr13 influencing the glomerulosclerosis**.** (C) The specific loci on Chr13 influencing glomerulosclerosis**.** The solid line represents genome-wide significance, and the dotted line represents suggestive. The x-axis shows the SNP loci ordered by distance along the chromosomes, chromosome 13, and focused on the specific loci of chromosome 13. The y-axis represents the -log(P-values). The SNP locus is indicated by an arrow.

## Supplementary Figure 5

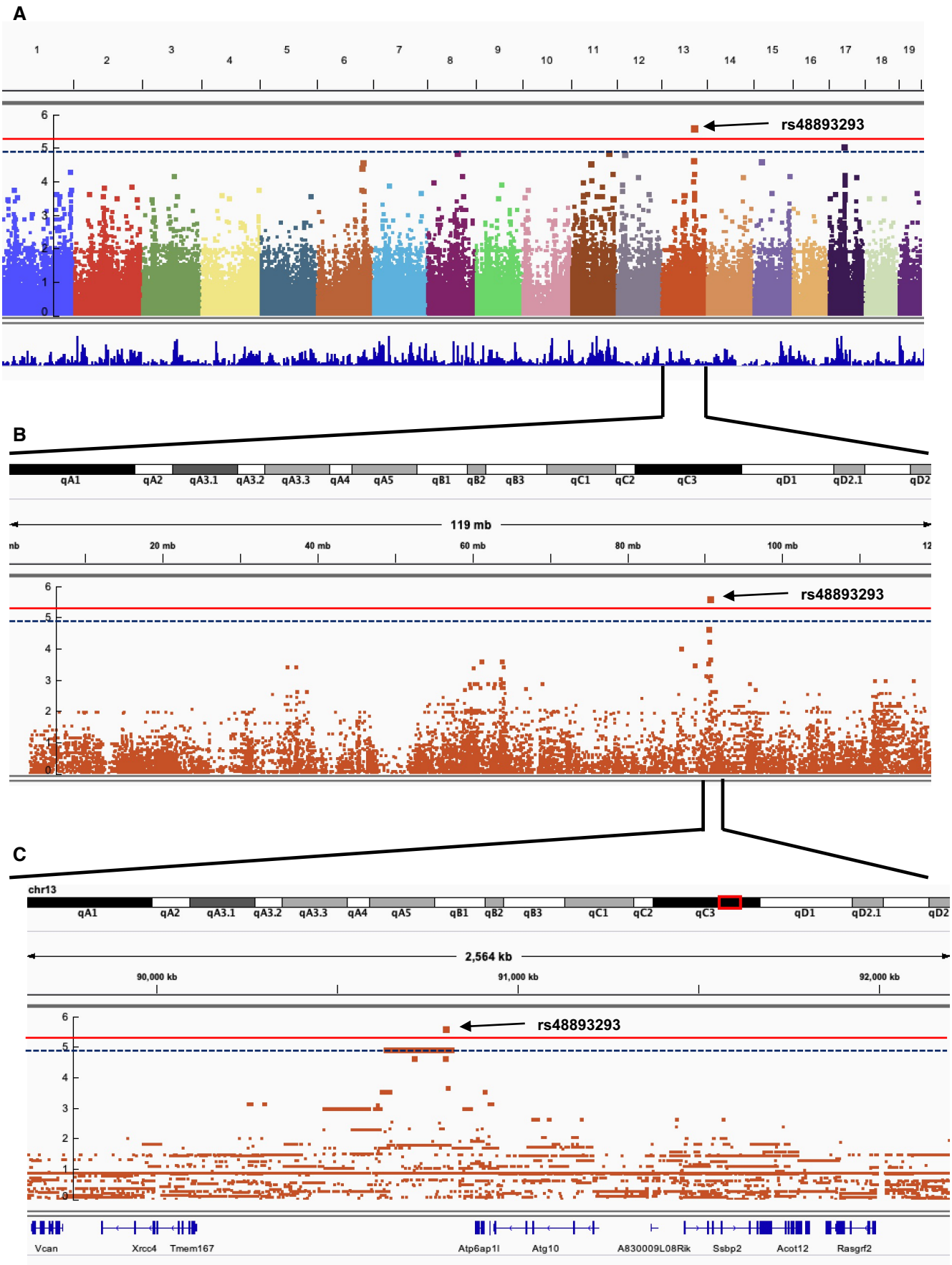

**Supplemental Figure 5: Manhattan plots for the loci influencing the casts phenotypes of the Tg-F1 mice.** (A) Manhattan plot of the percentage casts demonstrating a genome-wide significant SNP on Chr13. (B) Manhattan plot of Chr13 influencing casts**.** (C) The specific loci on Chr13 influencing casts**.** The solid line represents genome-wide significance, and the dotted line represents suggestive. The x-axis shows the SNP loci ordered by distance along the chromosomes, chromosome 13, and focused on the specific loci of chromosome 13. The y-axis represents the -log(P-values). The SNP locus is indicated by an arrow.

## Supplementary Figure 6

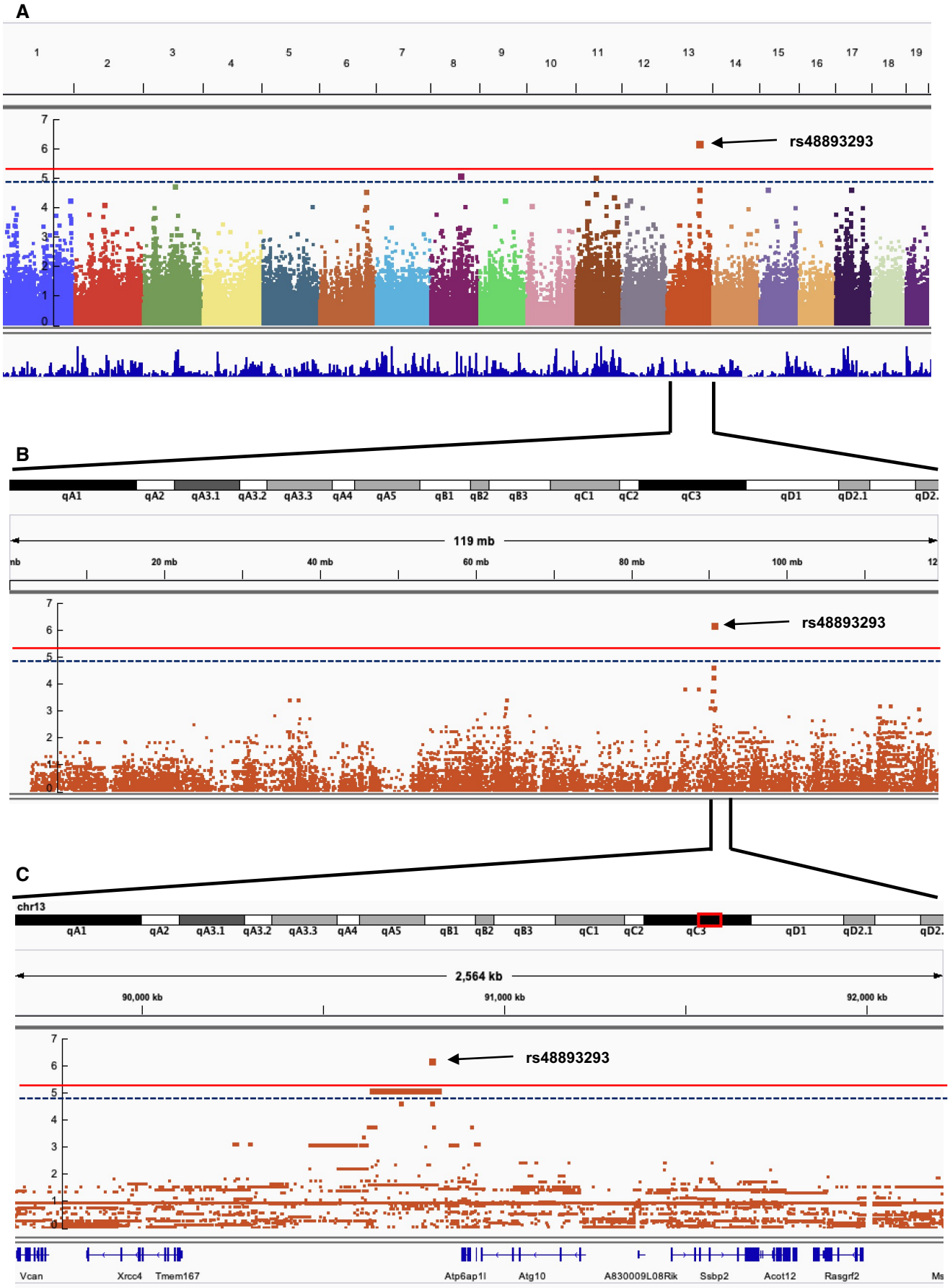

**Supplemental Figure 6: Manhattan plots for the loci influencing the tubular atrophy and interstitial fibrosis phenotypes of the Tg-F1 mice.** (A) Manhattan plot of the percentage TA/IF demonstrating a genome-wide significant SNP on Chr13. (B) Manhattan plot of Chr13 influencing tubular atrophy/interstitial fibrosis**.** (C) The specific loci on Chr13 influencing tubular atrophy/interstitial fibrosis**.** The solid line represents genome-wide significance, and the dotted line represents suggestive. The x-axis shows the SNP loci ordered by distance along the chromosomes, chromosome 13, and focused on the specific loci of chromosome 13. The y-axis represents the -log(P-values). The SNP locus is indicated by an arrow.

## Supplementary Figure 7

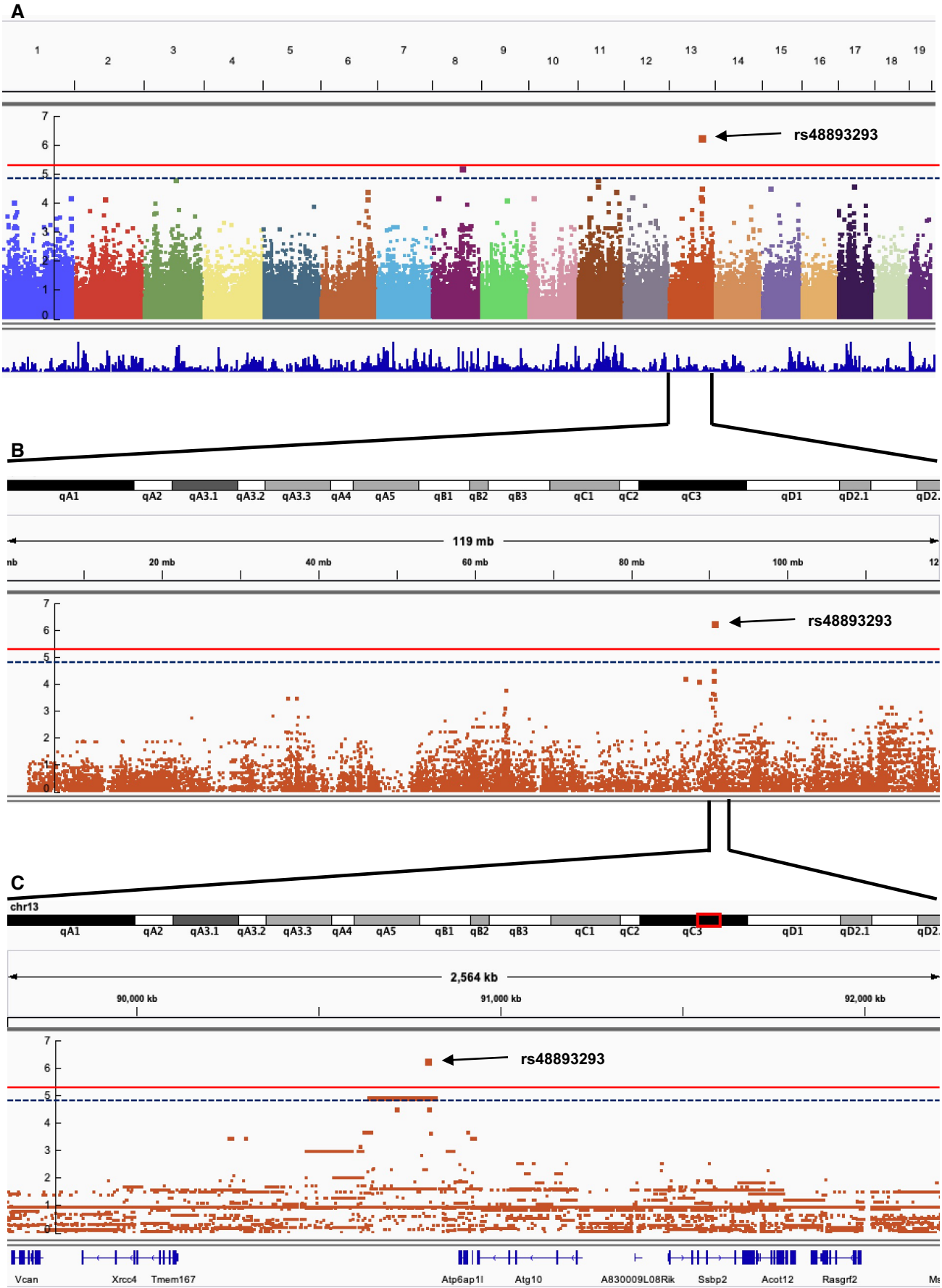

**Supplemental Figure 7: Manhattan plots for the loci influencing the interstitial inflammation phenotypes of the Tg-F1 mice.** (A) Manhattan plot of the percentage interstitial inflammation demonstrating a genome-wide significant SNP on Chr13. (B) Manhattan plot of Chr13 influencing interstitial inflammation. (C) The specific loci on Chr13 influencing interstitial inflammation. The solid line represents genome-wide significance, and the dotted line represents suggestive. The x-axis shows the SNP loci ordered by distance along the chromosomes, chromosome 13, and focused on the specific loci of chromosome 13. The y-axis represents the -log(P-values). The SNP locus is indicated by an arrow.

**Supplementary Figure 8**

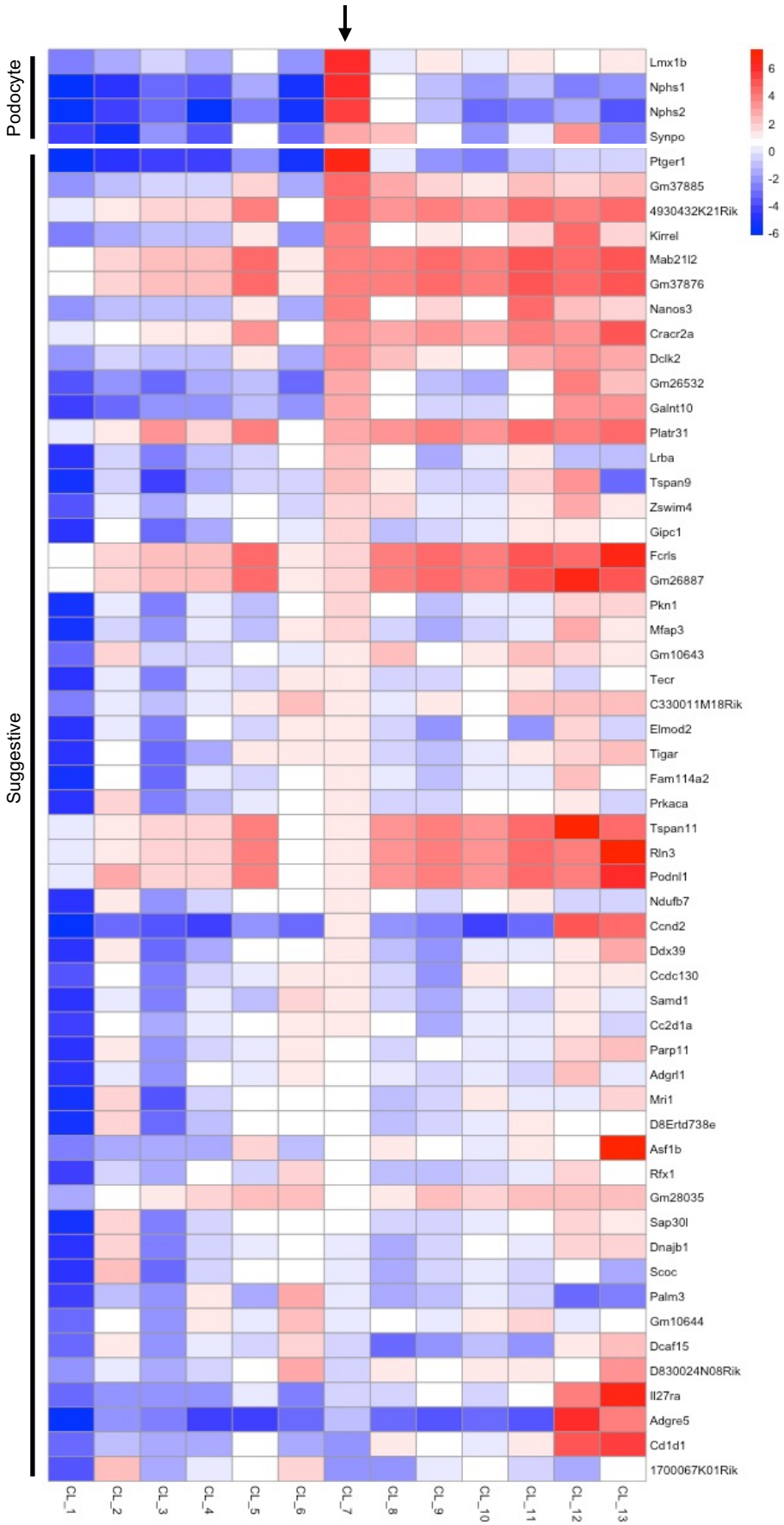

**Supplemental Figure 8: Differential expression of the genes located in suggestive loci.** Log2 fold change of differentially expressed genes identified in the suggestive loci using scRNA-Seq analysis, CL_7 contains podocyte specific genes including *Nphs1, Nphs2, Synpo, and Lmx1b.* Within the loci there are several genes that are significantly upregulated (Kirrel, Mab21l2, Cracr2a, Platr31, Nanos3 and Galnt10) in the gene cluster 7, containing the podocyte specific genes. CL-1 unknown, high mitochondrial content, CL_2 Proximal tubule, CL-3 Epithelial, CL_4 unknown, CL_5 Unknown, CL_6 Proximal tubule, CL_7 podocytes and Loop of Henle, CL_8 Collecting duct cells, CL_9 unknown, CL_10 Proximal tubule, CL_11 Loop of Henle, CL_12 Endothelial cells, CL_13 Macrophages and immune cells.

## Supplementary Figure 9

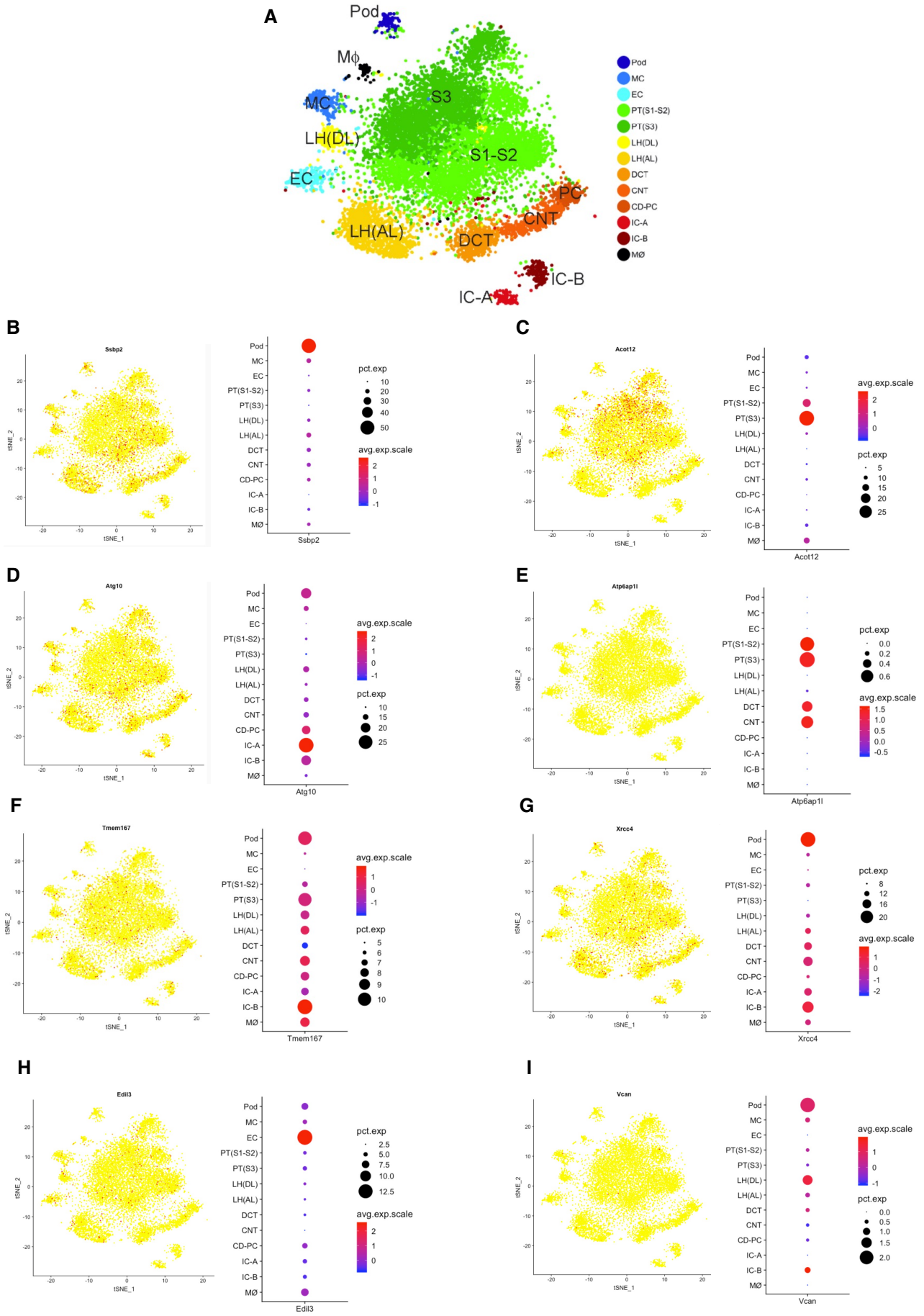

**Supplemental Figure 9: Mouse kidney tissue mRNA expression by snRNA-seq of the genes located in the identified locus on Chr. 13.**

(A) t_SNE plot of the cell population identified by the snRNA-seq. (B) *Ssbp2* gene expression in the kidney cell populations and *Ssbp2* is predominantly expressed in the podocytes. (C) *Acot12* gene expression in the kidney cell populations. (D) *Atg10* gene expression in the kidney cell populations. (E) *Atp6ap1l* gene expression in the kidney cell populations. (F) *Tmem167* gene expression in the kidney cell populations. (G) *Xrcc4* gene expression in the kidney cell populations. (H) *Edil3* gene expression in the kidney cell populations. (I) *Vcan* gene expression in the kidney cell populations. The snRNA-seq data was generated, analyzed, and visualized by the Humphreys Laboratory and downloaded from the KIT (Kidney interactive Transcriptomics) atlas at http://humphreyslab.com/SingleCell using the Healthy Mouse Dataset (Wu *et al* 2019, (S1)).

**Supplementary Figure 10**

**A** *SSBP2*

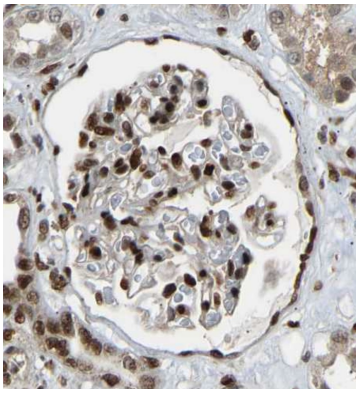

**B** *ATG10*

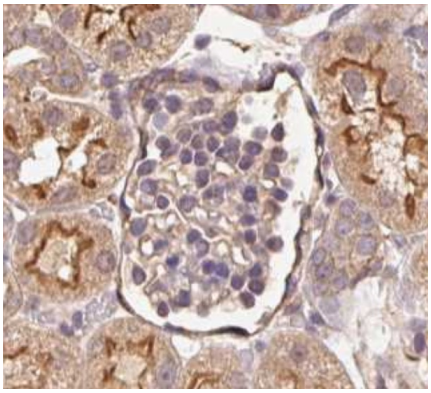

**C** *XRCC4*

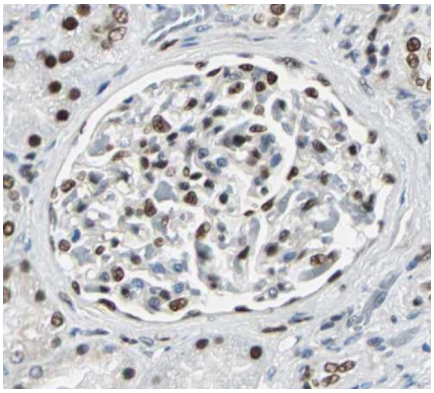

**D** *ATP6AP1L*

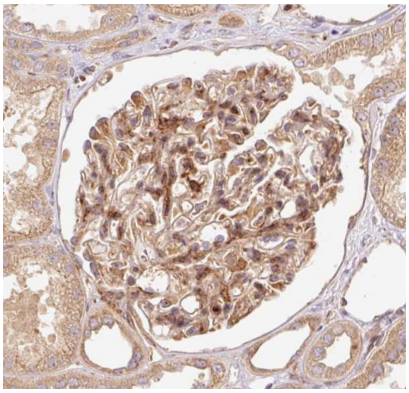

**Supplemental Figure 10: Immunostaining of kidney tissue of the genes identified in the QTL on chromosome 13.**

(A) SSBP2 staining in the kidney. (B) ATG10 staining in the kidney. (C) XRCC4 staining in the kidney. (D) ATP6AP1L staining in the human kidney. Images from Protein Atlas Database (69, 70).

## Supplementary Figure 11

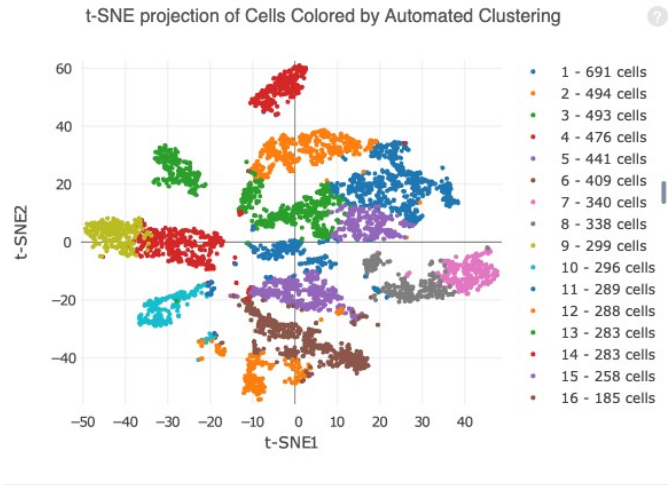


**HIVAN (TgFVB) kidneys**
1: Proximal Tubule
2: Proximal Tubule
3: Epithelial
4: Unknown
5: Loop of Henle
6: Loop of Henle
7: NK cells
8: T-cells
9: Unknown
10: Endothelial cells
11: B-cells
12: Collecting Duct cells
13: Macrophages and fibroblasts
14: Neutrophils
15: Unknown
16: Distal convoluted tubule.

**Supplemental Figure 11: Single cell sequencing of TgFVB kidney.**

Single cell sequencing of an HIV-1 transgenic mouse kidney derived from a TgFVB mouse demonstrates 16 distinct cell clusters**.** There are no clusters expressing podocyte specific genes.

**Supplementary Figure 12**

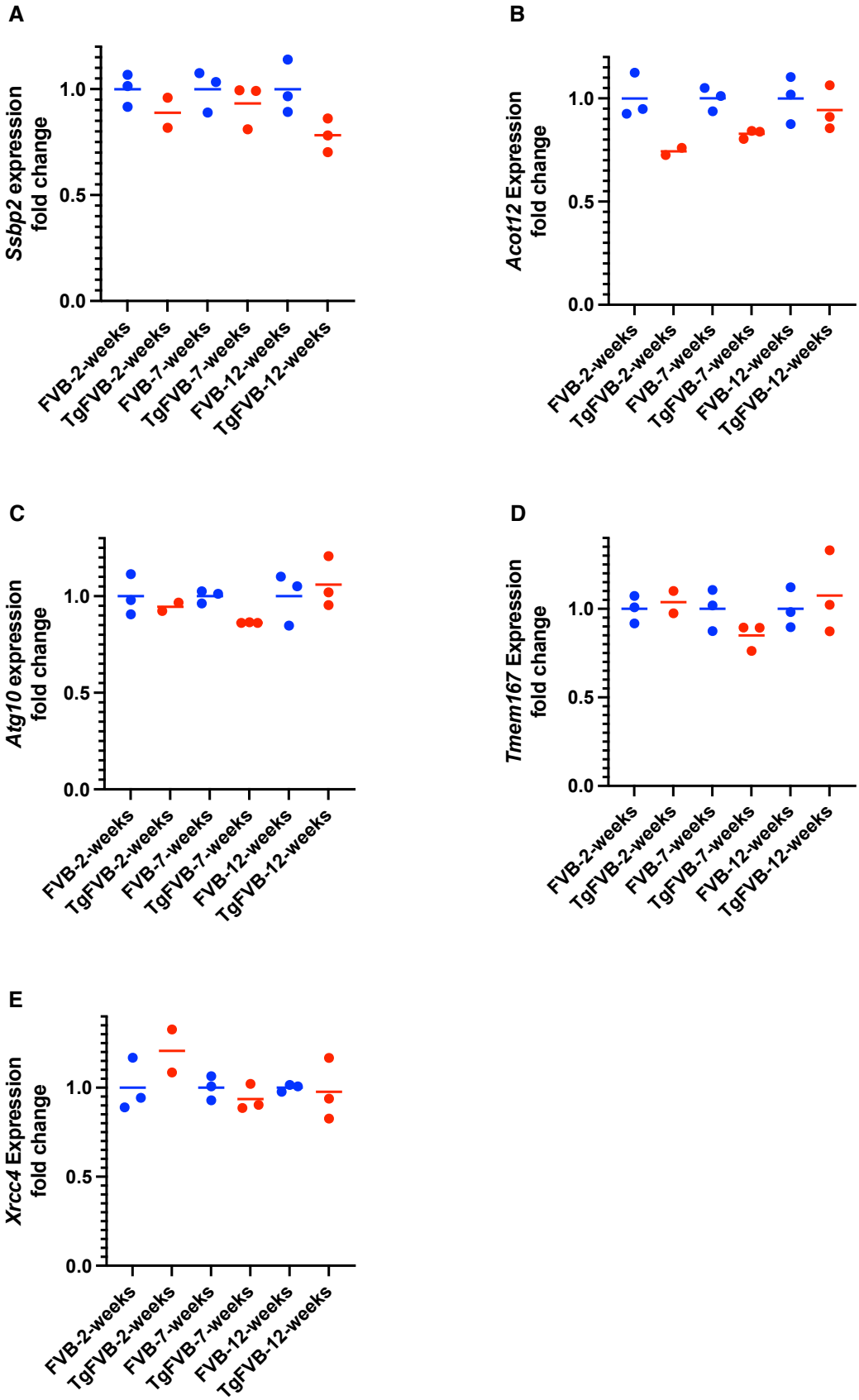

**Supplemental Figure 12: Quantitative RT-PCR analysis of genes identified within the Chr. 13 locus.**

(A) *Ssbp2* gene expression in FVB (blue dots) and TgFVB (red dots) mice at 2, 7 and 12 weeks of age. (B) *Acot12* gene expression in FVB (blue dots) and TgFVB (red dots) mice at 2, 7 and 12 weeks of age. (C) *Atg10* gene expression in FVB (blue dots) and TgFVB (red dots) mice at 2, 7 and 12 weeks of age. (D) *Tmem167* gene expression in FVB (blue dots) and TgFVB (red dots) mice at 2, 7 and 12 weeks of age. (E) *Xrcc4* gene expression in FVB (blue dots) and TgFVB (red dots) mice at 2, 7 and 12 weeks of age.

**Supplemental Table 1**: Numbers of Tg-F1-mice for each strain

| Tg-F1 mouse | Number |
|---|---|
| **129S1/SvImJ** | 24 |
| **A/J** | 8 |
| **BALB/cJ** | 25 |
| **C3H/HeJ** | 17 |
| **C57BL/10J** | 11 |
| **C57BL/6J** | 18 |
| **C57BL/6NJ** | 20 |
| **C57BL/J** | 17 |
| **C58/J** | 9 |
| **CAST/EiJ** | 7 |
| **CBA/J** | 18 |
| **DBA/1J** | 14 |
| **DBA/2J** | 12 |
| **KK/HiJ** | 13 |
| **LP/J** | 9 |
| **NOD/ShiLtJ** | 11 |
| **NZB/BINJ** | 17 |
| **NZO/HILtJ** | 12 |
| **WSB/EiJ** | 6 |
| **FVB/NJ** | 97 |

**Supplemental Table 2:** Primers for the RT-PCR.

| Gene | Forward Primer | Reverse Primer |
|---|---|---|
| **Beta-actin** | GGCTGTATTCCCCTCCATCG | CCAGTTGGTAACAATGCCATGT |
| **Ssbp2** | CAGGCCCGGGAGAAGTTAG | AGGTTTCCCGTCTCTCTGGA |
| **Atg10** | TCTGAAGTGACGAGACCTGC | GGAGCAGCCTCGGCTTATAG |
| **Vcan** | TGTCTGGAAAAGTGGTCCTACC | GACACTCGCCCCTTGTAGTC |
| **Xrcc4** | TCTCGGCATTTCTCCCTTGAG | CAGGTGCTCGTTTTTGGCTT |
| **Tmem167** | AGTCTGTTGACTGTAATCTTGCTG | GGCGACATAAGGACTCTTGC |
| **Acot12** | CAGTCCAGCCCACATAGCTT | GGCAGCACAACTGACCTTAG |

**Supplemental Table 3.** Statistical analysis of the glomerulosclerosis score between the different F1 hybrids compared to Tg-C57BL6/10J mice.

| Original FDR method of Benjamini and Hochberg | Mean rank diff. | Adjusted P value | P Value |
|---|---|---|---|
| **C57BL/10J-Tg vs. C57BL/6NJ-Tg** | -10.67 | 0.7746 | 0.7746 |
| **C57BL/10J-Tg vs. NZB.BINJ-Tg** | -53.08 | 0.1866 | 0.1669 |
| **C57BL/10J-Tg vs. CAST/EiJ-Tg** | -40.32 | 0.4231 | 0.4008 |
| **C57BL/10J-Tg vs. 129S1/SvImJ-Tg** | -64.07 | 0.0906 | 0.0763 |
| **C57BL/10J-Tg vs. C57BL/6J-Tg** | -68.96 | 0.0906 | 0.0695 |
| **C57BL/10J-Tg vs. C57L/J-Tg** | -70.89 | 0.0906 | 0.0763 |
| **C57BL/10J-Tg vs. BALB/cJ-Tg** | -91.27 | 0.0222 | 0.0152 |
| **C57BL/10J-Tg vs. C58/J-Tg** | -136.3 | 0.0027 | 0.0017 |
| **C57BL/10J-Tg vs. DBA/2J-Tg** | -130.5 | 0.0027 | 0.0016 |
| **C57BL/10J-Tg vs. NOD/ShiLtJ-Tg** | -140.5 | 0.0017 | 0.0009 |
| **C57BL/10J-Tg vs. NZO/HlLtJ-Tg** | -208.2 | <0.0001 | <0.0001 |
| **C57BL/10J-Tg vs. CBA/J-Tg** | -225.4 | <0.0001 | <0.0001 |
| **C57BL/10J-Tg vs. LP/J-Tg** | -237 | <0.0001 | <0.0001 |
| **C57BL/10J-Tg vs. WSB/EiJ-Tg** | -233.8 | <0.0001 | <0.0001 |
| **C57BL/10J-Tg vs. KK/HlJ-Tg** | -247.1 | <0.0001 | <0.0001 |
| **C57BL/10J-Tg vs. DBA/1J-Tg** | -258.5 | <0.0001 | <0.0001 |
| **C57BL/10J-Tg vs. C3H/HeJ-Tg** | -259.4 | <0.0001 | <0.0001 |
| **C57BL/10J-Tg vs. A/J-Tg** | -282.9 | <0.0001 | <0.0001 |
| **C57BL/10J-Tg vs. FVB/NJ-Tg** | -141.4 | <0.0001 | <0.0001 |

**Supplemental Table 4.** Statistical analysis of the glomerulosclerosis score between the different F1 hybrids compared to Tg-FVB/NJ mice.

| Original FDR method of Benjamini and Hochberg | Mean rank diff. | Adjusted P vlaue | P Value |
|---|---|---|---|
| FVB/NJ-Tg **vs.** C57BL/10J-Tg | 141.4 | <0.0001 | <0.0001 |
| FVB/NJ-Tg **vs.** C57BL/6NJ-Tg | 130.7 | <0.0001 | <0.0001 |
| FVB/NJ-Tg **vs.** NZB.BINJ-Tg | 88.29 | 0.0019 | 0.0007 |
| FVB/NJ-Tg **vs.** CAST/EiJ-Tg | 101.1 | 0.0147 | 0.0093 |
| FVB/NJ-Tg **vs.** 129S1/SvlmJ-Tg | 77.31 | 0.0019 | 0.0006 |
| FVB/NJ-Tg **vs.** C57BL/6J-Tg | 72.42 | 0.0094 | 0.0045 |
| FVB/NJ-Tg **vs.** C57L/J-Tg | 70.49 | 0.019 | 0.013 |
| FVB/NJ-Tg **vs.** BALB/cJ-Tg | 50.11 | 0.0525 | 0.0442 |
| FVB/NJ-Tg **vs.** C58/J-Tg | 5.107 | 0.9256 | 0.8769 |
| FVB/NJ-Tg **vs.** DBA/2J-Tg | 10.85 | 0.8058 | 0.721 |
| FVB/NJ-Tg **vs.** NOD/ShiLtJ-Tg | 0.8294 | 0.979 | 0.979 |
| FVB/NJ-Tg **vs.** NZO/HILtJ-Tg | -66.78 | 0.0353 | 0.0279 |
| FVB/NJ-Tg **vs.** CBA/J-Tg | -84.05 | 0.0023 | 0.001 |
| FVB/NJ-Tg **vs.** LP/J-Tg | -95.67 | 0.0108 | 0.0057 |
| FVB/NJ-Tg **vs.** WSB/EiJ-Tg | -92.44 | 0.0353 | 0.0268 |
| FVB/NJ-Tg **vs.** KK/HIJ-Tg | -105.7 | 0.0112 | 0.0065 |
| FVB/NJ-Tg **vs.** DBA/1J-Tg | -117.2 | 0.0002 | <0.0001 |
| FVB/NJ-Tg **vs.** C3H/HeJ-Tg | -118 | 0.0007 | 0.0002 |
| FVB/NJ-Tg **vs.** A/J-Tg | -141.6 | 0.0005 | 0.0001 |

**Supplemental Table 5.** Statistical analysis of the casts score between the different F1 hybrids compared to Tg-C57BL6/10J mice.

| Original FDR method of Benjamini and Hochberg | Mean rank diff. | Adjusted P value | P Value |
|---|---|---|---|
| C57BL/10J-Tg **vs.** C57BL/6NJ-Tg | -6.445 | 0.8627 | 0.8627 |
| C57BL/10J-Tg **vs.** NZB.BINJ-Tg | -64.96 | 0.1079 | 0.0908 |
| C57BL/10J-Tg **vs.** CAST/EiJ-Tg | -45.26 | 0.3649 | 0.3457 |
| C57BL/10J-Tg **vs.** 129S1/SvlmJ-Tg | -54.32 | 0.1485 | 0.1329 |
| C57BL/10J-Tg **vs.** C57BL/6J-Tg | -67.85 | 0.0939 | 0.0741 |
| C57BL/10J-Tg **vs.** C57L/J-Tg | -82.8 | 0.0522 | 0.0384 |
| C57BL/10J-Tg **vs.** BALB/cJ-Tg | -101.9 | 0.0098 | 0.0067 |
| C57BL/10J-Tg **vs.** C58/J-Tg | -140.1 | 0.0021 | 0.0012 |
| C57BL/10J-Tg **vs.** DBA/2J-Tg | -140.2 | 0.0014 | 0.0007 |
| C57BL/10J-Tg **vs.** NOD/ShiLtJ-Tg | -121.7 | 0.0064 | 0.004 |
| C57BL/10J-Tg **vs.** NZO/HILtJ-Tg | -207 | <0.0001 | <0.0001 |
| C57BL/10J-Tg **vs.** CBA/J-Tg | -219.7 | <0.0001 | <0.0001 |
| C57BL/10J-Tg **vs.** LP/J-Tg | -257.4 | <0.0001 | <0.0001 |
| C57BL/10J-Tg **vs.** WSB/EiJ-Tg | -242.7 | <0.0001 | <0.0001 |
| C57BL/10J-Tg **vs.** KK/HIJ-Tg | -234.2 | <0.0001 | <0.0001 |
| C57BL/10J-Tg **vs.** DBA/1J-Tg | -264.9 | <0.0001 | <0.0001 |
| C57BL/10J-Tg **vs.** C3H/HeJ-Tg | -244 | <0.0001 | <0.0001 |
| C57BL/10J-Tg **vs.** A/J-Tg | -284.9 | <0.0001 | <0.0001 |
| C57BL/10J-Tg **vs.** FVB/NJ-Tg | -131.4 | <0.0001 | <0.0001 |

**Supplemental Table 6.** Statistical analysis of the casts score between the different F1 hybrids compared to Tg-FVB/NJ mice.

| Original FDR method of Benjamini and Hochberg | Mean rank diff. | Adjusted P value | P Value |
|---|---|---|---|
| FVB/NJ-Tg **vs.** C57BL/10J-Tg | 131.4 | 0.0001 | <0.0001 |
| FVB/NJ-Tg **vs.** C57BL/6NJ-Tg | 125 | <0.0001 | <0.0001 |
| FVB/NJ-Tg **vs.** NZB.BINJ-Tg | 66.49 | 0.0187 | 0.0109 |
| FVB/NJ-Tg **vs.** CAST/EiJ-Tg | 86.19 | 0.036 | 0.0265 |
| FVB/NJ-Tg **vs.** 129S1/SvlmJ-Tg | 77.13 | 0.0016 | 0.0007 |
| FVB/NJ-Tg **vs.** C57BL/6J-Tg | 63.6 | 0.0187 | 0.0126 |
| FVB/NJ-Tg **vs.** C57L/J-Tg | 48.65 | 0.1095 | 0.0865 |
| FVB/NJ-Tg **vs.** BALB/cJ-Tg | 29.51 | 0.2804 | 0.2361 |
| FVB/NJ-Tg **vs.** C58/J-Tg | -8.698 | 0.7919 | 0.7919 |
| FVB/NJ-Tg **vs.** DBA/2J-Tg | -8.723 | 0.7919 | 0.774 |
| FVB/NJ-Tg **vs.** NOD/ShiLtJ-Tg | 9.766 | 0.7919 | 0.7572 |
| FVB/NJ-Tg **vs.** NZO/HlLtJ-Tg | -75.6 | 0.0187 | 0.0128 |
| FVB/NJ-Tg **vs.** CBA/J-Tg | -88.24 | 0.0014 | 0.0005 |
| FVB/NJ-Tg **vs.** LP/J-Tg | -126 | 0.001 | 0.0003 |
| FVB/NJ-Tg **vs.** WSB/EiJ-Tg | -111.3 | 0.0155 | 0.0077 |
| FVB/NJ-Tg **vs.** KK/HlJ-Tg | -102.7 | 0.0155 | 0.0082 |
| FVB/NJ-Tg **vs.** DBA/1J-Tg | -133.4 | <0.0001 | <0.0001 |
| FVB/NJ-Tg **vs.** C3H/HeJ-Tg | -112.5 | 0.0012 | 0.0004 |
| FVB/NJ-Tg **vs.** A/J-Tg | -153.5 | 0.0001 | <0.0001 |

**Supplemental Table 7.** Statistical analysis of the tubular atrophy and interstitial fibrosis score between the different F1 hybrids compared to Tg-C57BL6/10J mice.

| Original FDR method of Benjamini and Hochberg | Mean rank diff. | Adjusted P value | P Value |
|---|---|---|---|
| C57BL/10J-Tg **vs.** C57BL/6NJ-Tg | -2.989 | 0.9355 | 0.9355 |
| C57BL/10J-Tg **vs.** NZB.BINJ-Tg | -61.95 | 0.123 | 0.1036 |
| C57BL/10J-Tg **vs.** CAST/EiJ-Tg | -33.44 | 0.5088 | 0.482 |
| C57BL/10J-Tg **vs.** 129S1/SvlmJ-Tg | -65.36 | 0.0861 | 0.068 |
| C57BL/10J-Tg **vs.** C57BL/6J-Tg | -51.95 | 0.1873 | 0.1676 |
| C57BL/10J-Tg **vs.** C57L/J-Tg | -74.36 | 0.0822 | 0.0606 |
| C57BL/10J-Tg **vs.** BALB/cJ-Tg | -98.34 | 0.0122 | 0.0083 |
| C57BL/10J-Tg **vs.** C58/J-Tg | -129.4 | 0.0049 | 0.0026 |
| C57BL/10J-Tg **vs.** DBA/2J-Tg | -113.5 | 0.009 | 0.0057 |
| C57BL/10J-Tg **vs.** NOD/ShiLtJ-Tg | -119.1 | 0.0078 | 0.0045 |
| C57BL/10J-Tg **vs.** NZO/HILtJ-Tg | -197.6 | <0.0001 | <0.0001 |
| C57BL/10J-Tg **vs.** CBA/J-Tg | -211.8 | <0.0001 | <0.0001 |
| C57BL/10J-Tg **vs.** LP/J-Tg | -245.9 | <0.0001 | <0.0001 |
| C57BL/10J-Tg **vs.** WSB/EiJ-Tg | -220.4 | <0.0001 | <0.0001 |
| C57BL/10J-Tg **vs.** KK/HIJ-Tg | -230.1 | <0.0001 | <0.0001 |
| C57BL/10J-Tg **vs.** DBA/1J-Tg | -254.9 | <0.0001 | <0.0001 |
| C57BL/10J-Tg **vs.** C3H/HeJ-Tg | -243.8 | <0.0001 | <0.0001 |
| C57BL/10J-Tg **vs.** A/J-Tg | -265.6 | <0.0001 | <0.0001 |
| C57BL/10J-Tg **vs.** FVB/NJ-Tg | -103.7 | 0.0019 | 0.0009 |

**Supplemental Table 8.** Statistical analysis of the tubular atrophy and interstitial fibrosis score between the different F1 hybrids compared to Tg-FVB/NJ mice.

| Original FDR method of Benjamini and Hochberg | Mean rank diff. | Adjusted P value | P Value |
|---|---|---|---|
| FVB/NJ-Tg **vs.** C57BL/10J-Tg | 103.7 | 0.0024 | 0.0009 |
| FVB/NJ-Tg **vs.** C57BL/6NJ-Tg | 100.7 | 0.0001 | <0.0001 |
| FVB/NJ-Tg **vs.** NZB.BINJ-Tg | 41.75 | 0.1445 | 0.1064 |
| FVB/NJ-Tg **vs.** CAST/EiJ-Tg | 70.27 | 0.1076 | 0.0679 |
| FVB/NJ-Tg **vs.** 129S1/SvlmJ-Tg | 38.34 | 0.1276 | 0.0873 |
| FVB/NJ-Tg **vs.** C57BL/6J-Tg | 51.76 | 0.0697 | 0.0403 |
| FVB/NJ-Tg **vs.** C57L/J-Tg | 29.34 | 0.3759 | 0.2968 |
| FVB/NJ-Tg **vs.** BALB/cJ-Tg | 5.367 | 0.8278 | 0.8278 |
| FVB/NJ-Tg **vs.** C58/J-Tg | -25.71 | 0.5122 | 0.4313 |
| FVB/NJ-Tg **vs.** DBA/2J-Tg | -9.785 | 0.7865 | 0.7451 |
| FVB/NJ-Tg **vs.** NOD/ShiLtJ-Tg | -15.43 | 0.6951 | 0.6219 |
| FVB/NJ-Tg **vs.** NZO/HlLtJ-Tg | -93.87 | 0.0038 | 0.0018 |
| FVB/NJ-Tg **vs.** CBA/J-Tg | -108.1 | <0.0001 | <0.0001 |
| FVB/NJ-Tg **vs.** LP/J-Tg | -142.2 | 0.0001 | <0.0001 |
| FVB/NJ-Tg **vs.** WSB/EiJ-Tg | -116.7 | 0.0091 | 0.0048 |
| FVB/NJ-Tg **vs.** KK/HlJ-Tg | -126.4 | 0.0024 | 0.001 |
| FVB/NJ-Tg **vs.** DBA/1J-Tg | -151.2 | <0.0001 | <0.0001 |
| FVB/NJ-Tg **vs.** C3H/HeJ-Tg | -140.1 | <0.0001 | <0.0001 |
| FVB/NJ-Tg **vs.** A/J-Tg | -161.8 | <0.0001 | <0.0001 |

**Supplemental Table 9.** Statistical analysis of the interstitial inflammation score between the different F1 hybrids compared to Tg-C57BL6/10J mice.

| Original FDR method of Benjamini and Hochberg | Mean rank diff. | Adjusted P value | P Value |
|---|---|---|---|
| C57BL/10J-Tg **vs.** C57BL/6NJ-Tg | -18.88 | 0.6106 | 0.6106 |
| C57BL/10J-Tg **vs.** NZB.BINJ-Tg | -58.5 | 0.1495 | 0.1259 |
| C57BL/10J-Tg **vs.** CAST/EiJ-Tg | -32.05 | 0.53 | 0.5022 |
| C57BL/10J-Tg **vs.** 129S1/SvlmJ-Tg | -65.24 | 0.0922 | 0.0697 |
| C57BL/10J-Tg **vs.** C57BL/6J-Tg | -51.52 | 0.1933 | 0.1729 |
| C57BL/10J-Tg **vs.** C57L/J-Tg | -71.41 | 0.0922 | 0.0728 |
| C57BL/10J-Tg **vs.** BALB/cJ-Tg | -93.2 | 0.0187 | 0.0128 |
| C57BL/10J-Tg **vs.** C58/J-Tg | -127 | 0.0062 | 0.0033 |
| C57BL/10J-Tg **vs.** DBA/2J-Tg | -106.4 | 0.0157 | 0.0099 |
| C57BL/10J-Tg **vs.** NOD/ShiLtJ-Tg | -116.6 | 0.0097 | 0.0056 |
| C57BL/10J-Tg **vs.** NZO/HILtJ-Tg | -193.6 | <0.0001 | <0.0001 |
| C57BL/10J-Tg **vs.** CBA/J-Tg | -210.5 | <0.0001 | <0.0001 |
| C57BL/10J-Tg **vs.** LP/J-Tg | -250.2 | <0.0001 | <0.0001 |
| C57BL/10J-Tg **vs.** WSB/EiJ-Tg | -221 | <0.0001 | <0.0001 |
| C57BL/10J-Tg **vs.** KK/HIJ-Tg | -230.1 | <0.0001 | <0.0001 |
| C57BL/10J-Tg **vs.** DBA/1J-Tg | -255.8 | <0.0001 | <0.0001 |
| C57BL/10J-Tg **vs.** C3H/HeJ-Tg | -245.9 | <0.0001 | <0.0001 |
| C57BL/10J-Tg **vs.** A/J-Tg | -267.6 | <0.0001 | <0.0001 |
| C57BL/10J-Tg **vs.** FVB/NJ-Tg | -127.1 | 0.0001 | <0.0001 |

**Supplemental Table 10.** Statistical analysis of the interstitial inflammation score between the different F1 hybrids compared to Tg-FVB/NJ mice.

| Original FDR method of Benjamini and Hochberg | Mean rank diff. | Adjusted P value | P Value |
|---|---|---|---|
| FVB/NJ-Tg **vs.** C57BL/10J-Tg | 127.1 | 0.0003 | <0.0001 |
| FVB/NJ-Tg **vs.** C57BL/6NJ-Tg | 108.2 | <0.0001 | <0.0001 |
| FVB/NJ-Tg **vs.** NZB.BINJ-Tg | 68.63 | 0.0142 | 0.0082 |
| FVB/NJ-Tg **vs.** CAST/EiJ-Tg | 95.08 | 0.022 | 0.0139 |
| FVB/NJ-Tg **vs.** 129S1/SvlmJ-Tg | 61.89 | 0.0127 | 0.006 |
| FVB/NJ-Tg **vs.** C57BL/6J-Tg | 75.61 | 0.0068 | 0.0029 |
| FVB/NJ-Tg **vs.** C57L/J-Tg | 55.72 | 0.0614 | 0.0485 |
| FVB/NJ-Tg **vs.** BALB/cJ-Tg | 33.93 | 0.203 | 0.1709 |
| FVB/NJ-Tg **vs.** C58/J-Tg | 0.1716 | 0.9958 | 0.9958 |
| FVB/NJ-Tg **vs.** DBA/2J-Tg | 20.76 | 0.55 | 0.4921 |
| FVB/NJ-Tg **vs.** NOD/ShiLtJ-Tg | 10.49 | 0.7795 | 0.7384 |
| FVB/NJ-Tg **vs.** NZO/HlLtJ-Tg | -66.45 | 0.0379 | 0.0279 |
| FVB/NJ-Tg **vs.** CBA/J-Tg | -83.42 | 0.0027 | 0.001 |
| FVB/NJ-Tg **vs.** LP/J-Tg | -123.1 | 0.0011 | 0.0004 |
| FVB/NJ-Tg **vs.** WSB/EiJ-Tg | -93.86 | 0.0349 | 0.0239 |
| FVB/NJ-Tg **vs.** KK/HlJ-Tg | -103 | 0.0142 | 0.0077 |
| FVB/NJ-Tg **vs.** DBA/1J-Tg | -128.6 | <0.0001 | <0.0001 |
| FVB/NJ-Tg **vs.** C3H/HeJ-Tg | -118.8 | 0.0006 | 0.0002 |
| FVB/NJ-Tg **vs.** A/J-Tg | -140.5 | 0.0005 | 0.0001 |

**Supplemental Table 11**: Estimated heritability for the kidney pathology scores and BUN

| Trait | h |
|---|---|
| **BUN** | 0.49 |
| **GS** | 0.87 |
| **Casts** | 0.78 |
| **TA/IF** | 0.83 |
| **Int/Infl** | 0.82 |

**h** = heritability values range from 0 to 1.

**Supplemental Table 12:** Suggestive signals (Chromosome Wide Significant) of the glomerulosclerosis scores from the HIV-1 transgenic mice. Genes expressed in the podocyte are in bold text.

| Chr | Peak Pos (Mb) | Peak SNP | Confidence Interval (Mb) | LOD | Genes within confidence intervals |
|---|---|---|---|---|---|
| **3** | 87.28 | rs212172476 | 87.286-87.287 | 3.71 | Cd1d1, Cd1d2, **Dclk2**, Fcrls, **Kirrel**, Lrba, **Mab21l2** |
| **6** | 128.05 | rs52540263 | 128.052-128.053 | 3.63 | Ccnd2, **Cracr2a**, Fgf23, Parp11, **Platr31**, Prmt8, Tigar, Tpi-rs11, Tspan11, Tspan9 |
| **8** | 84.28 | rs579631690 | 84.281-84.282 | 3.91 | Adgre5, Adgrl1, Asf1b, Cc2d1a, Ccdc130, Clgn, Dcaf15, Ddx39, Dnajb1, Elmod2, Gipc1, Il27ra, Mgat4d, Misp3, Mri1, **Nanos3**, Ndufb7, Olfr370, Palm3, Pkn1, Podnl1, Prkaca, Ptger1, Rfx1, Rln3, Samd1, Scoc, Tecr, Ucp1, Zswim4 |
| **11** | 57.89 | rs52098593 | 57.89-57.9 | 4.0 | Fam114a2, **Galnt10**, Gria1, Hand1, Mfap3, n-R5s69, Sap30l |
| **15** | 24.8 | 15:24803781-C-G | 24.803-24.804 | 3.76 | none |

**Supplemental Table 13:** Selection of priority genes in the locus identified on Chr.13. The priority genes were chosen based on the protein expression in the glomerulus and the single cell gene expression in podocytes. Genes highlighted in red are the priority genes.

| Gene | Predicted gene | Protein atlas expression | Single Cell Seq expression in podocytes | Mouse Models | Known interactions with kidney disease genes | GWAS catalog associations (p<10-8) |
|---|---|---|---|---|---|---|
| ***Gm34585*** | Yes | N/A | N/A | N/A | N/A | N/A |
| ***Edil3*** | No | High in tubules | No | No phenotypic data described | No | Major depressive disorder, Protein quantitative trait loci (liver), CSF Hyaluronan and proteoglycan link protein 1 |
| ***Gm34699*** | Yes | N/A | N/A | N/A | N/A | N/A |
| ***Vcan*** | No | Not detected | No | Defects in the heart. Embryonic lethal at day 10.5 | No | White matter microstructure, appendicular lean mass, body fat distribution, carotid artery intima media thickness, brain volume measurement |
| ***Xrcc4*** | No | Glomerulus | Yes | Embryonic lethal at day 17.5 | No | Heel bone mineral density, White matter microstructure, Squamous cell lung carcinoma |
| ***Tmem167*** | No | No protein tissue data | Yes | Decreased circulating triglyceride and total protein level | No | Aspartate aminotransferase levels in non-alcoholic fatty liver disease, Male-pattern baldness, Cortical surface area |
| ***Gm35111*** | Yes | N/A | N/A | N/A | N/A | N/A |
| ***Atp6ap1l*** | No | Tubules and glomerulus | No | No phenotypic data described | No | Carotid intima media thickness, Breast cancer, Serum alkaline phosphatase levels, General cognitive ability, DNA methylation variation (age effect), Self-reported math ability (MTAG), red cell distribution width |
| ***Atg10*** | No | Tubules | Yes | No phenotypic data described | No | Airway imaging phenotypes, Breast cancer, Self-reported math ability, Adventurousness |
| ***Gm41014*** | Yes | N/A | N/A | N/A | N/A | N/A |

| | | | | | | |
|---|---|---|---|---|---|---|
| ***A80009L08Rik*** | Yes | N/A | N/A | N/A | N/A | N/A |
| ***Ssbp2*** | No | Glomerulus and tubules | Yes | lymphoma and carcinoma. Kidney FSGS phenotype. | LMX1B | Body mass index, Predicted visceral adipose tissue, Bipolar disorder, Adolescent idiopathic scoliosis, Adult body size, General cognitive ability, platelet count, Toxicity response to radiotherapy in prostate cancer, educational achievement, Cortical surface area |
| ***4833422C13Rik*** | Yes | N/A | N/A | N/A | N/A | N/A |
| ***Acot12*** | No | No protein tissue data | Yes, very few cells | No phenotypic data described | No | None |

Supplemental Reference:

S1. Wu H, Kirita Y, Donnelly EL, Humphreys BD: Advantages of Single-Nucleus over Single-Cell RNA Sequencing of Adult Kidney: Rare Cell Types and Novel Cell States Revealed in Fibrosis. *J Am Soc Nephrol,* 30**:** 23-32, 2019 10.1681/ASN.2018090912